ACROSS-SCALE TEMPERATURE MODELLING USING A SIMPLE APPROACH FOR THE CHARACTERIZATION OF HIGH MOUNTAIN ECOSYSTEM COMPLEXITY

With 6 figures and 1 supplement (III)

JÖRG LÖFFLER and ROLAND PAPE

Zusammenfassung: Skalenübergreifende Temperaturmodellierung unter Verwendung eines einfachen Ansatzes zur Charakterisierung der Ökosystemkomplexität im Hochgebirge

Ein einfacher Modellierungsansatz wurde zur Charakterisierung der Komplexität von Hochgebirgsökosystem verwendet, um die Dynamik der oberflächennahen Temperaturen zu simulieren. Die Heterogenität der untersuchten Landschaft führte zu einem skalenübergreifenden Vorgehen, das die vertikalen Interaktionen am Standort (Nano-Skala), die kleinräumige Differenzierung innerhalb von Einzugsgebieten (Mikro-Skala) und den Höhenstufenwandel eines gesamten Gebirgsmassivs (Meso-Skala) verknüpfte. Das Modell wurde anhand detaillierter Messungen an verschiedenen Standorten kalibriert. Nach einer Modellvalidierung mit Daten sehr hoher zeitlicher Auflösung waren die Simulationsläufe zufrieden stellend. In allen Fällen konnte das Modell die Varianz der gemessenen Temperaturen mit einer Genauigkeit von über 80% erklären. Nachfolgend wurden Korrelationen zwischen generellen meteorologischen Trends und der mikroklimatischen Differenzierung untersucht. Die Hypothese war, dass übergeordnete Witterungsverläufe als meteorologische Phänomene ihre Entsprechung in der mikroklimatischen Situation (v.a. in der Dynamik der oberflächennahen Temperaturen) finden und somit für die Steuerung der ökosystemaren Funktionsweise verantwortlich gemacht werden können. Die Ergebnisse zeigten jedoch, dass die kleinräumigen Verhältnisse ihren Ausdruck in komplexen Grundzügen des Temperaturwandels entlang großräumiger Höhengradienten finden. Der generell zur Beschreibung der Höhenwandels herangezogene adiabatische Koeffizient konnte deshalb nicht zur Interpretation des vorgefundenen ökosystemaren Wirkungsgefüges verwendet werden. Die Abweichungen zwischen den Messwerten und den allgemeinen Annahmen wurden in Korrelationsmatrizen aufgezeigt. Schließlich konnte die Komplexität der ökosystemaren Steuerung durch den Energiehaushalt mit Hilfe von Temperaturgradienten erklärt werden, die durch eine skalenübergreifende Multiregressionsanalyse ermittelt wurden. Es wurde somit gezeigt, unter welchen raum-zeitlichen Rahmenbedingungen und mit welchen Abweichungen die standörtlichen Verhältnisse den generellen meteorologischen Annahmen entsprechen.

Summary: A modelling approach was practised to characterize the complexity of high mountain ecosystems using a new simple model to simulate near-surface temperature variations. The heterogeneity of the investigated landscape led to an across-scale procedure that combined vertical interactions at single locations (nano-scale), micro-spatial differentiations within small catchments (micro-scale), and altitudinal changes of an entire mountain system (meso-scale). The model was calibrated on detailed measurements for different sites. Simulation runs were satisfactory according to model validation based on data with high temporal resolution. In all cases, more than 80% of the variance of observed temperatures was explained by the model. We analysed correlations between general meteorological trends and local climatic differentiations. The hypothesis was that different overlying meteorological phenomena (i.e. different weather situations) would find their expression in micro-climatic conditions (especially in the variation of near-surface temperatures) superiorly determining ecosystem functioning. It turned out that the micro-spatial conditions resulted in complex principles of thermal changes along altitudinal broad-scale gradients. So, the adiabatic lapse rate, commonly used to describe the altitudinal zonation, did not explain the different mosaics of ecosystems. We illustrated the biases between measurements and common assumptions by means of correlation matrices. To conclude, the complexity of the ecosystem determining energy balance was described by complex differences of temperature gradients that were achieved from across scale multi-regression analysis. It was shown to which degree local site conditions corresponded with meteorological assumptions under different spatio-temporal conditions.

1 Introduction

1.1 Complexity in northern high mountains

Northern high mountain landscapes above the timberline show diverse micro-spatial patterns of ecosystems that function most heterogeneously according to interaction and combination of different environmental parameters (KÖRNER 1995; MOSIMANN 1985; SHAVER a. JONASSON 1999). Steep meteorological and topographical gradients, as well as altitudinal zonation and complex relief micro-features, most decisively affect the alpine ecology (BILLINGS 1973; KUDO et al. 1999; JONES et al. 2001). Those gradients are complex and their impact on the environment is not yet fully understood (KÖRNER 1999). With their focus on Fennoscandian alpine vegetation many case studies have been conducted very early (e.g. documented by PÅHLSSON

1994). Since little is known about environmental conditions and vegetation patterns at higher elevations (FREMSTAD 1997), however, the scientific challenge in mountain geography of northern Europe is still to intensify research on fine-scale temperature and snow cover determinants, and superior broad-scale oceanic-continental gradients (FÆGRI 1972). Consequently, convictions on the environmental determination of the northern high mountain vegetation could be scrutinized as to new results of a long-term landscape ecological project (KÖHLER et al. 1994).

1.2 Across-scale concept

The concept of multiple scales was adopted to the northern mountain areas (LÖFFLER 2002a) using landscape ecological terminology (BASTIAN a. STEINHARDT 2002) derived from the *theory of geographical dimensions* (NEEF 1967). Landscape complexes were used in a hierarchical order combined with corresponding scale terms, principally based on a transition of emergence moving from one spatial level of abstraction to another (LÖFFLER 2002b).

Some explanations of the determination of high mountain ecosystems that dominate literature were found insufficient regarding different spatial scales (LÖFFLER 2003). The fine-scale topography was supposed to impact upon the vegetation within two major causal chains (DAHL 1956; BILLINGS 1973; MAY 1976; MOLENAAR 1987; ISARD a. BELDING 1989; WALKER et al. 2001). Simplified, these chains are: a) exposed site – thin snow cover – strong prevailing winds – enforced evapotranspiration – lack of soil moisture – drought stress – cold winters but long vegetation period, and b) lee slope – thick snow cover – shelter against winds and low temperatures – sufficient supply of water but short vegetation period. By quantifying soil moisture and micro-climate variability we showed that a lack in water availability was not found at any time. Instead, complex spatio-temporal temperature gradients affected the vegetation superiorly (LÖFFLER 2004).

Moreover, the altitudinal gradient across the alpine belts had been explained by temperature and precipitation means corresponding with specific changes in the vegetation (FÆGRI 1972; MYKLESTAD 1993; HUGGETT 1995; VIRTANEN et al. 1999). So, higher elevations had principally been understood as being under harder environmental conditions (GJÆREVOLL 1990; FREMSTAD 1997). Our results on micro-climatic determination of the vegetation gave evidence that higher precipitation resulted in earlier and thicker sheltering snow cover at higher elevations. Hence, the lowest temperatures were found at lower altitudes as to inversions, where snow cover was thinnest and frost damage was most affecting (LÖFFLER 2003). All in all, the results showed that vegetation was above all determined by prevailing near-surface temperature variations resulting from complex factor constellations at different sites (LÖFFLER 2002a).

As shown in figure 1, thermoisopleth diagrams were used to illustrate the complex daily and annual variations of near-surface temperatures. Three layers were analysed, air temperature at 15 cm height above ground (referred to as T+15 hereafter), sub-surface temperature measured at 1 cm depth below ground (referred to as T–1 hereafter), and substrate temperature at 15 cm depth below ground (referred to as T–15 hereafter). These were chosen for site comparison along topographical gradients, micro-spatial ecotope type characterization, and broad-scale analysis of altitudinal changes. The three near-surface temperature layers were analysed as to their synchronicity (by means of r^2, defined as the variance of one curve explained by another) and their deviation (by means of RMSE, defined as a measure of deviation) against the standard meteorological air temperatures at 2 m height (referred to as T+200 hereafter). Figure 1 schematically explains 13 different ecological processes combined with dominant temperature conditions near ground over time (LÖFFLER a. WUNDRAM 2001). With this diagram we explained both vertical temperature profiles and spatial temperature differentiations: these differed extraordinarily within a fine-scale focus and statistically corresponded significantly with the distribution of plant species and vegetation types (LÖFFLER 2003). In addition, spatial near-surface temperature differentiations were particularly supposed to determine abundances of epigeic arthropods (OTTESEN 1996).

Combining investigations in different catchments along altitudinal gradients resulted in a process-oriented geographical comparison of alpine landscapes (LÖFFLER a. WUNDRAM 2003). Spatial extrapolation into broader scales combined with regionalization approaches were supported with a simple model that simulated spatial temperature variations on the basis of field measurements in a wider net (PAPE a. LÖFFLER 2004). Within the ecosystem approach of this long-term project, across-scale concepts were needed to quantify biogeochemical cycles and energy fluxes in catchments and to regionalize the results into larger areas as also expressed by WITHERS and MEENTEMEYER (1999).

1.3 Modelling approach

Regional and local climate are controlling factors with regard to ecosystem functioning (FREMSTAD 1997),

but the assessment of meteorological data is a general problem in high mountain research, since most official meteorological stations are located in the valleys (PRICE a. BARRY 1997). Consequently, common approaches of spatial data interpolation (HUTCHINSON 1995; FLEMING et al. 2000) are critical due to the general lack of data from higher elevations. Furthermore, a simple but common approach to assess altitudinal gradients is based on the adiabatic lapse rate of temperature (WHITEWAY et al. 1995). In such approaches the (mean) air temperature at two metres height above ground is used. But, its ecological relevance seemed to be ques-

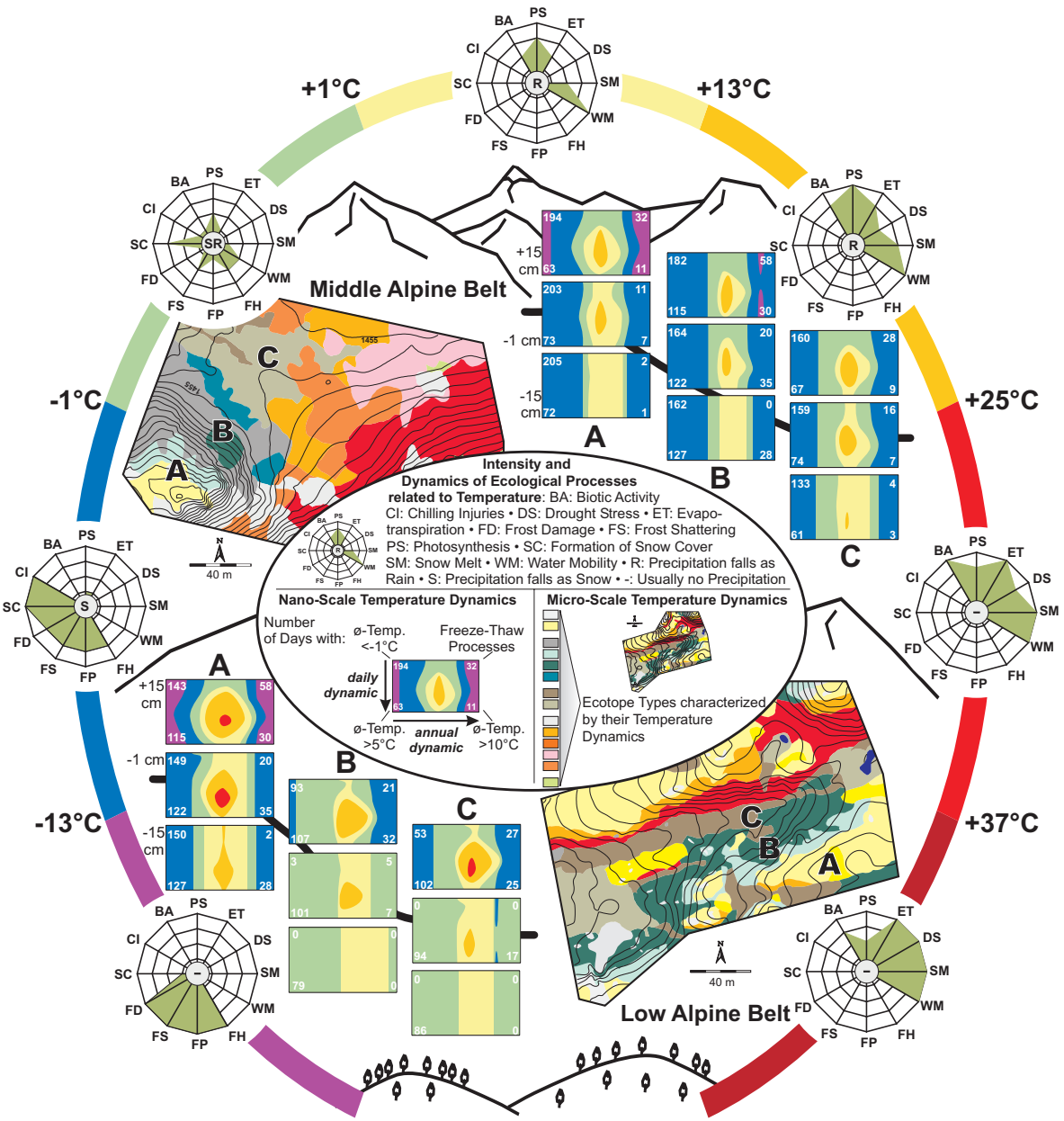

Fig. 1: Across-scale concept for the characterization of high mountain ecosystems along vertical site specific, topographical, and altitudinal gradients (Orig.)

Skalenübergreifendes Konzept zur Charakterisierung von Hochgebirgsökosystemen entlang vertikaler standortspezifischer, topographischer und höhenwärtiger Gradienten

tionable, especially in high mountain landscapes where vegetation cover seldom extends beyond heights of one metre (LESER 1997).

Numerical models for operational weather prediction cover a wide range of scales accomplished by general circulation models (GCM) and their down-scaling (RUMMUKAINEN et al. 2001; DENBY et al. 2002). Models appropriate for these scales cannot resolve fine-scale differentiations conditioned by the complex high mountain topography (NOPPEL a. FIEDLER 2002). The results are important deficiencies in prediction, for boreal and tundra landscapes generally reinforced by "at best incomplete and at worst incorrect" representation of the land surface (HARDING et al. 2001, 15).

Identifying the interface between land surface and atmosphere as the key area in reducing uncertainties in prediction has led to the development of one-dimensional soil-vegetation-atmosphere-transfer (SVAT) models (JANSSON a. KARLBERG 2001; CAYROL et al. 2000). These enable pretty exact simulations of energy fluxes and temperatures, but are subject to the general problem of their applicability (BOULET et al. 2000): Especially when they exhibit small time and space steps, they are difficult to use for the investigation of the spatial and temporal variability of land surface fluxes. The large number of parameters they involve requires detailed field studies and experimentation to derive parameter estimates. Thus, running such models on each point location is intractable.

In addition, the transition of scales exhibits a gap between micro-scale 1D models neglecting lateral processes and macro-scale 3D GCMs. This gap is only basically bridged by spatial meso-scale models for specific landscapes (e.g. BRUSE 1999). As opposed to this, water balance models cover a wide range of scales (BRONSTERT a. PLATE 1997; ARNOLD et al. 1998).

Consequently, we developed a suitable 1D, spatially fine-scaled numerical model for the energy balance of high mountain ecosystems that was used as a basis for across scale modelling from catchment to altitudinal zonation (PAPE a. LÖFFLER 2004).

Applying models to smaller map scales facilitates the approach of regionalization resulting in generalized spatial data for the sake of high local accuracy. Such geographically based procedures enable spatio-temporal modelling of ecosystem functioning for different scales (KRYSANOVA et al. 1999; BRONSTERT et al. 2001).

1.4 Aims and objectives

This paper deals with high mountain landscapes of Norway, methods to analyse spatial patterns and dynamics of alpine ecosystems, and a modelling approach to simulate superior processes that determine their functioning principles. The primary aim of this study was to assess the significance of simple standard methods dealing with temperature interpolation along topographical and altitudinal gradients (e.g. the adiabatic lapse rate). We supposed meteorological phenomena such as specific events during different weather situations to find their expression in micro-spatial climatic conditions such as local near-surface temperature profiles. Thus, the secondary aim was to quantify these superior determinants of high mountain ecosystem complexity. Eventually, the tertiary aim of this project was to model high resolution spatio-temporal patterns of high mountain landscapes and to predict their determining dynamics.

2 Area descriptions, methods, techniques

2.1 Area description

As a consequence of the north-southward stretch of the Scandes, central Norway shows a clearly defined oceanic-continental gradient between western and eastern slopes of the mountain chain. The most continental climate is found only 150 km east off the coast in the Vågå/Oppland region (61° 53′ N; 9° 15′ E). The study area situated within this climatic region is characterized by a lowest annual precipitation of about 300–400 mm per year (in the valleys), i.e. showing the highest aridity found in Norway. The alpine altitudinal zonation is differentiated into a low-alpine belt, dominated by shrub and heather communities, and a middle-alpine belt, dominated by grassy vegetation (DAHL 1986). It reaches from the tree-line at about 1,000–1,050 m a.s.l. to the highest peak, the Blåhø, with 1,618 m a.s.l. The entire mountain massif above the tree-line comprises an area of roughly 50 km^2. The transition zone between low- and middle-alpine belts is found at around 1,350 m a.s.l. (Fig. 2).

2.2 Methods and techniques of field investigation and data analysis

Small characteristic catchments were delimited in each altitudinal belt. The two catchments were mapped and measurements were transposed from representative sites into space. Figure 3 illustrates the topographical structure of the study sites, the spatial organization of measurements, parameters measured as well as the use of technical equipment at the different types of stations. The arrangement followed premises on weighing the highest spatial resolution possible, the most quanti-

tative results measurable, by the lowest priced instruments available. In each catchment one ecological base station, several major and minor ecological stations as well as numerous water level stations were installed. Seasonal ecosystem dynamics was assessed by means of measurements taken throughout the year at hourly intervals by data loggers, registering air and soil temperature, precipitation, solar radiation, air humidity, soil moisture, wind direction, and wind speed. Spatial differentiations of temperature, soil moisture, and wind speed were investigated using hand-held measurements at various locations during several characteristic climatic situations and seasons. Additional data were received from the NORWEGIAN METEOROLOGICAL INSTITUTE (1991–2002) comprising of long-term measurements at the official station Kjøremsgrende Nr. 16740 (1976) (Lesja, Oppland) at 626 m a.s.l.

Resulting data were organized digitally in a data base, combined and structured into a GIS for spatial analysis. Mapped spatial data layers, such as vegetation types, relief features, snow cover conditions etc., were used to define structural ecotope types by overlay rou-

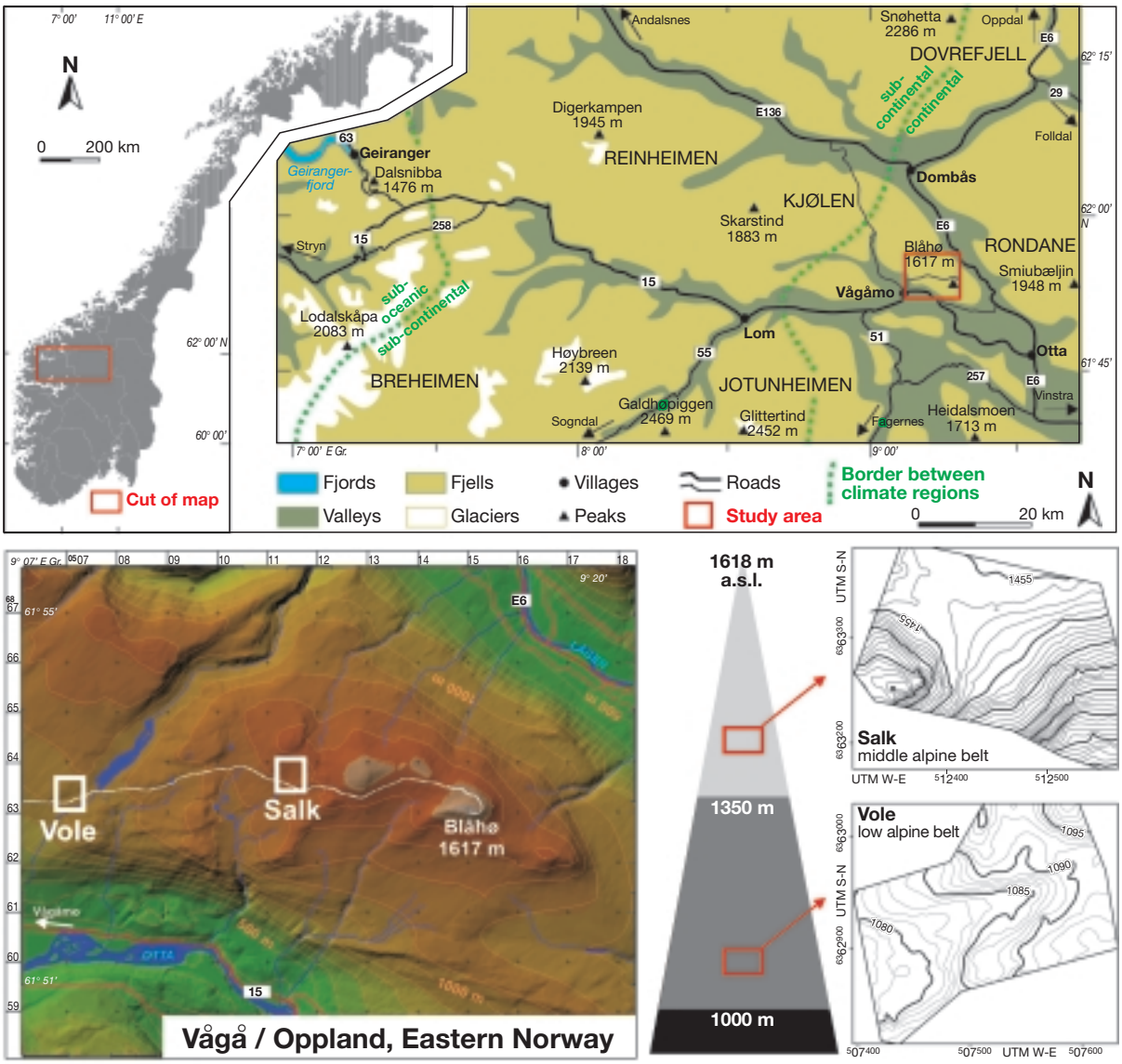

Fig. 2: Location and topography of the study area in central Norway (Orig.)

Lage und Topographie des Untersuchungsraums in Mittelnorwegen

tines. Ecotopes were defined as quasi-homogeneous areas that function with regard to different ecological factors (LESER 1997), being analogous to the hydrological response units used in hydrology (FLÜGEL 1996).

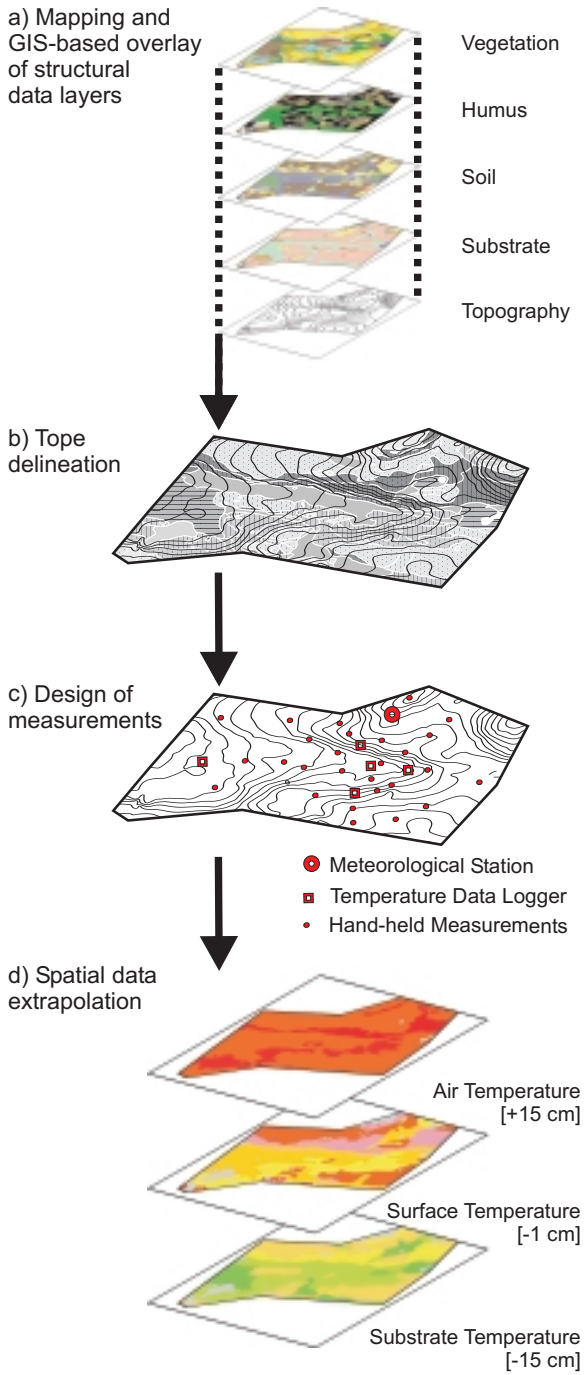

Fig. 3: Spatial organisation of investigations (Orig.)
Räumliche Organisation der Untersuchungen

These highly integrating tope-type geometries determined the position of measurements based on four hierarchical levels of stations and functioned as spatial basis for data extrapolation. Ecological regularities statistically deduced from all functional data were quantified and generalized for each catchment.

2.3 Modelling approach and model implementation

Near-surface temperature variations at a site were calculated according to the modelling approach of PAPE and LÖFFLER (2004). Balancing the energy fluxes at the surface led to a high temporal resolution of temperatures based on a set of physical equations (Fig. 4). The resulting one-dimensional, vertically structured energy balance model represents temperature variations within an air layer of two metres height above a layered soil profile covered with vegetation. Meteorological standard data were used as driving forces in the model and were given as measured values.

As discussed above, common SVAT models use a high amount of input data for accurate estimations of surface fluxes. To avoid time-consuming and labour-intensive determinations of empirical variables, only input data easy to deduce were used within this model. Consequently, simulation of near-surface temperature dynamics was based on:

– mappings of site-dependent structures as relief (controlling height above sea level, aspect, inclination), substrate (mineral, organic) and vegetation type (determining stand height, leaf area index, albedo), and their derivation from remote sensing, respectively,

– measurements of time-dependent variables ("driving forces") as global radiation, air temperature, and wind speed at 2 m height, relative humidity, precipitation, barometric pressure, and

– calculations of the spatial distribution of actual and maximum possible radiation depending on the relief (FU a. RICH 1999).

Besides the output of air temperature, sub-surface temperature, and substrate temperature, the governing sensible, latent, and ground heat fluxes also served as output data. Moreover, the water equivalent of the latent heat flux was used to estimate potential evaporation.

Model calculations were implemented using spreadsheets. The internal model structure consisted of seven compartments: 1) database of site-dependent environmental factors, 2) time series of dynamic input factors, 3) calculation routines of vegetation surface temperature, i.e. solving its energy balance by iteration, 4) calculation routines of ground surface temperature, again by solving its energy balance by iteration, 5) calculation

of substrate temperature, 6) air temperature, and finally 7) resulting time series of calculated values. The results were visualized by spreadsheet routines and imported into a GIS for spatial analysis and extrapolation.

The surface temperature as the driving force for heat fluxes, within both the air and the substrate, needed to be estimated first as the basis for further calculations. It was deduced from the balance between the energy fluxes at the surface. Each flux was broken down into constituent parts and formed a complete equation set consisting of net-radiation (R_n), evaporative flux (H_L), sensible heat flux (H_S), and ground heat flux (H_G), which was resolved to obtain the surface temperature.

The net available radiant energy (R_n) was found to consist of two components: the absorbed solar flux at the surface (R_s) depending on global radiation R_{glo}, the relief, and the albedo of the surface (A, given as fraction) supposed to be independent of sun angle. The second component was the net long-wave flux (L_n) based on the temperature difference between the surface and the overlying medium according to the Stefan-Boltzmann-Law. The amount of solar radiation absorbed at the substrate surface (subscript sfc) not only depends on albedo but also on properties of the covering vegetation canopy (subscript c) expressed according to SCHELDE (1996, 8) by an empirical constant (C = 0.5) and the leaf

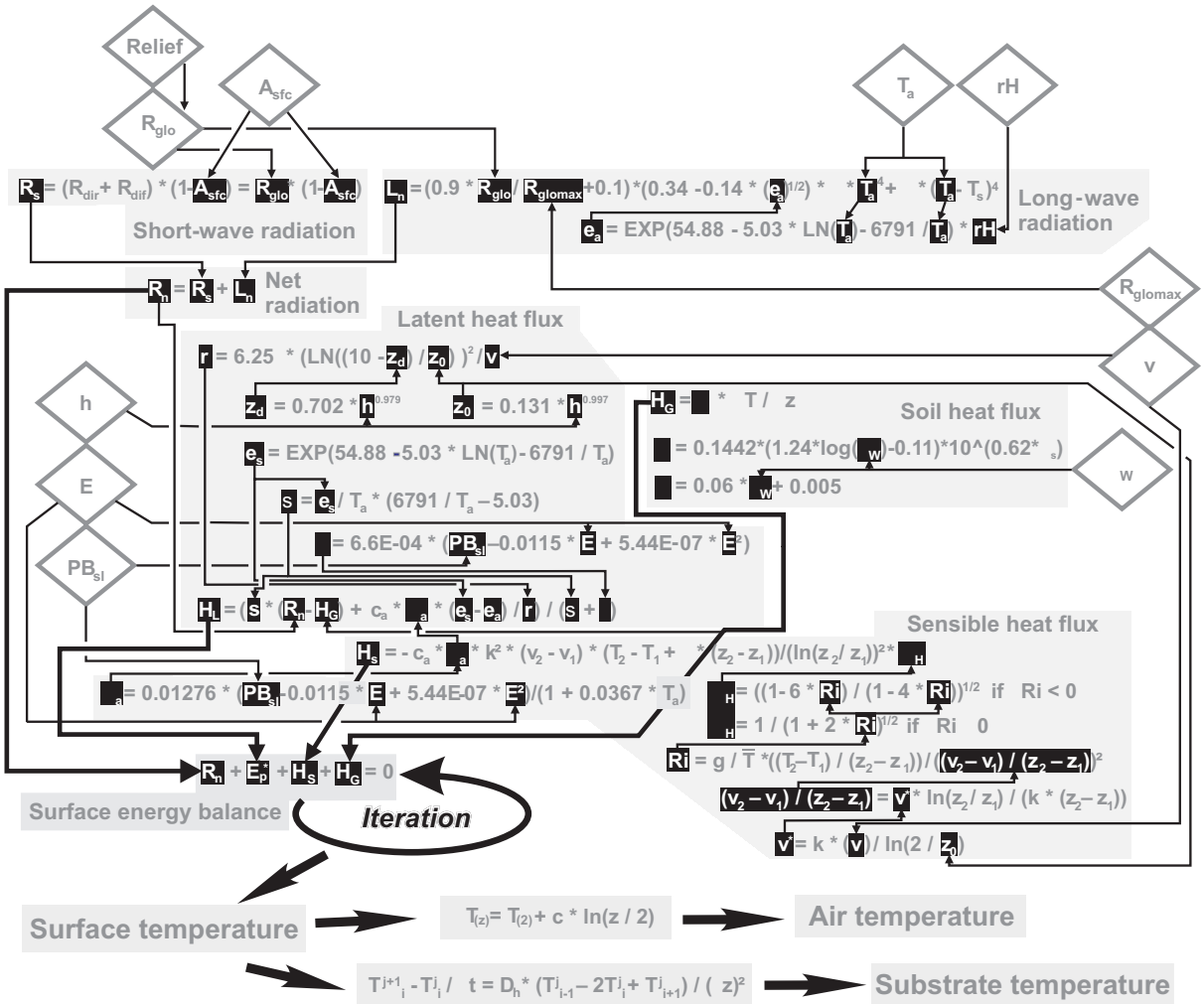

Fig. 4: Architecture of the superior 1D energy balance model, explanations are given within the text (after: LÖFFLER a. PAPE 2003)

Architektur des übergeordneten 1D-Energiehaushaltsmodells; nähere Erläuterungen im Text

area index LAI supposed to be 0–2.5 according to BLISS et al. (1981).

Regarding the canopy surface, the net long wave flux was more complex because of interactions with the atmosphere. According to KONDRATYEV (1969) a correction term for the actual vapour pressure of the air was included (e_a, MITCHELL et al. 1997: Eq. 52, 53), and an approximation of cloud cover (MITCHELL et al. 1997: Eq. 58) was used by the ratio between actual global radiation R_{glo} and calculated maximum possible global radiation R_{glomax} (FU a. RICH 1999). During night times when no global radiation was measured, cloud cover until midnight was roughly estimated from the mean ratio R_{glo}/R_{glomax} during the last three hours before sunset and afterwards from the mean ratio during three hours after sunrise. Due to the small spatial extent of the investigated catchments (each less than 5 hectares), spatial variability of cloudiness was neglected.

Relative humidity (rH) was used as fraction, and e_s as the saturation vapour pressure [hPa] at actual air temperature in 2 m (T_a) calculated according to MITCHELL et al. (1997: Eq. 52). The net radiation itself was balanced by the upward flux of sensible heat (H_S) into the atmosphere, the heat flux into the ground (H_G) and the latent heat flux (H_L) into the atmosphere.

The flux of sensible heat was calculated using an aerodynamic approach mentioned by FLEAGLE and BUSINGER (1963, 195), where c_a was the specific heat of air (1,009 $Jkg^{-1}K^{-1}$, OKE, 2001, 44), ρ_a the density of air [kgm^{-3}], k the Karman constant (0.41), v wind velocity [ms^{-1}], T temperature, Γ the adiabatic lapse rate of temperature (9.72 10^{-3} km^{-1}) and z the height of measurement. To consider the stability of the atmosphere and to account for a wider applicability of the profile method, generally being restricted to neutral stability of the atmosphere, a stability function for heat (Φ_H) according to BRUSE and FLEER (1998) was included, depending on the Richardson number Ri (OKE 2001, 380). PB_{sl} represented the barometric pressure at sea level [hPa], and E, the elevation of the site [m]. g was the acceleration due to gravity (ms^{-2}), T with subscript, the temperature at the measurement heights z_1 and z_2, T without subscript, the mean of these two values and v, wind velocity at the two heights z_1 and z_2. In the above-mentioned equations the subscripts 1 and 2 referred to the surface itself and the vegetation canopy in case of the substrate surface to be regarded, otherwise they referred to the canopy surface and the air at 2 m.

This aerodynamic approach required measurements of both vertical temperature and wind velocity gradients. As wind velocity was measured continuously at a height of two metres only, its vertical profile had to be estimated. According to OKE (2001, 381) the wind velocity gradient between 2 m and the canopy surface as well as between both surfaces was estimated using the friction velocity (v^*) with h being the height of the vegetation canopy.

Ground heat flux H_G [Wm^{-2}] was expressed by H_G, with λ as the thermal conductivity of substrate [$Wm^{-1}K^{-1}$], ΔT, the temperature difference between surface and first measurement point within substrate and Δz, the depth of the first measurement point within substrate. For unfrozen mineral substrates an empirical conductivity function was adapted from KERSTEN (1949) where c_1, c_2, c_3 were constants depending on whether the substrate was dominated by clay, silt or sand, θ_w described the volumetric water content [%], and ρ_s was the dry bulk density of the substrate [gcm^{-3}]. For the predominating silty sand the following parameterization was used: $c_1 = 1.24$, $c_2 = -0.11$, $c_3 = 0.62$, $\rho_s = 1.6$. Thermal conductivity of organic matter was estimated by a function adapted from DE VRIES (1975).

Latent heat flux H_L [Wm^{-2}] was calculated according to Penman as reported in MITCHELL et al. (1997) for a saturated surface, where s was the slope of the saturation vapour pressure curve [10^3 PaK^{-1}], γ the psychrometer constant [10^3 PaK^{-1}], and r the aerodynamic resistance [sm^{-1}]. Considering water to become limiting and actual evaporation to become less than potential, a simple approach was used assuming water being equally available throughout the entire soil water range, but not accessible at the permanent wilting point TANNER (1967). As continuous measurements of soil moisture at the driest sites within the study areas indicated, the water content was constantly higher than at the permanent wilting point (LÖFFLER 2002a). For simplification the actual latent heat flux was assumed to be equal to the potential heat flux.

The only remaining unknown quantity within the energy flux equations was the surface temperature enabling the equation system to be solved according to the temperature of both substrate surface and canopy surface. A numerical solution was prevented, because many parameters were indirectly or directly related to the surface temperature itself. The solution was found by iterations as to *regula falsi* (BRUSE a. FLEER 1997):

a) Two initial surface temperature values (T^0 and T^1) were chosen. For T^0 the temperature of the former time step was used; T^1 set to be $T^0 + 0.2$.

b) These two temperatures were used to calculate the energy balance resulting in two balance values F^0 and F^1.

c) Inserting these two values yielded a new value T^2 for the surface temperature.

d) It was set $T^0 = T^1$ and $T^1 = T^2$; steps b) and c) were repeated until the convergence criterion $|T^1 - T^0| \leq 0.001$ K was reached.

The canopy surface temperature was calculated first, using the substrate surface temperature of the former time step. Then the result was used to calculate a new substrate surface temperature and vice versa. As such, the definite temperature was found by iteration.

The substrate layer was assumed to have homogenous thermal properties. Using a backward difference scheme provided by HANKS and ASHCROFT (1980), it was possible to approximate the non-steady state heat flux equation numerically, where the subscripts i referred to depth increments, Δz distance apart, and the superscripts j referred to the time increments, Δt time apart, and D_h being the thermal diffusivity (in 10^{-6} m^2s^{-1}) of the substrate given for silty sand and for organic matter separately.

The air temperature was assumed to decrease (at night) or increase (at daytime) logarithmically with height (GEIGER 1961, 82-84), where c was an empirical constant. It was estimated for c and using the modelled temperature of the vegetation surface and measured T+200. Thus, the air temperature at every height was calculated, where the superscript z referred to the unknown air temperature at the height z and the superscript 1 referred to T+200.

2.4 Model Calibration and Validation

The model was calibrated for different sites, including lichen heath-covered ridge positions, mid slopes covered by dwarf shrub heath, and depressions with mire vegetation using measured temperatures. The site-dependent parameters albedo and LAI were then adjusted by minimizing the difference between observed and calculated surface temperature for 168 data points. This approach was used because the initial settings were not measured but taken from literature. Nevertheless, adjustments were made within a realistic range given in literature.

The goodness of temperature representation after minimizing was tested against independent hourly temperature measurements throughout fourteen days. It was presented using root mean square errors (hereafter referred to as RMSE) as well as r^2-values of a linear regression:

– r^2, as $\left(\frac{n(\sum XY) - (\sum X)(\sum Y)}{\sqrt{[n\sum X^2 - (\sum X)^2]\ [n\sum Y^2 - (\sum Y)^2]}}\right)^2$

– RMSE, as $\sqrt{\frac{\sum (X-Y)^2}{n}}$

3 Results

The results were based on a fourteen-day summer period of representative measurements and model calculations illustrated by means of temperature curves derived from hourly means (Suppl. III). After that, a comparison of four different layers of temperatures was practiced on the nano-scale: I, air temperature T+200, II, air temperature T+15, III, sub-surface temperature T–1, and IV, substrate temperature T–15. Furthermore, three different sites along micro-spatial topographical gradients were compared on the micro-scale: A, ridge position, B, mid-slope position (north-facing), and C, depression. Finally, comparing the low- and middle-alpine belts, general altitudinal trends were assessed on the meso-scale. These comparisons were all based on measured temperatures.

The different steps of across-scale modelling and comparison were presented in 14 diagrams showing temperature curves to assess the model quality and to demonstrate the detailed variation of temperatures, as well as the following three types of correlation matrices:
– nano-scale: I, II, III, and IV
– micro-scale: A, B, and C
– meso-scale: low-alpine, and middle-alpine

As such, Supplement I illustrates the local temperature variation near ground, the relief-determined differentiation of energetic site conditions, and the adiabatic lapse rate of temperatures with altitude. Figure 5 is used to sum up the general results of the adiabatic temperature biases during different weather situations.

3.1 Model accuracy

The model explained more than 80% ($r^2 \geq 0.805$) of the variance of observed temperatures combined with low biases (RMSE ≤ 1.448) for all regarded sites and layers within the low and middle alpine belts. So, no further setbacks were necessary to fit the model. Best accuracy was found regarding soil temperatures ($r^2 \geq 0.91$, RMSE ≤ 0.59), except the low alpine depression with higher biases. Worst biases ($r^2 \leq 0.89$, RMSE ≥ 0.87) were observed for the sub-surface temperature, except the low alpine ridge with better accuracy. The air temperature was intermediate. We used the measured values for the following comparisons.

3.2 Nano-scale results

Vertical temperature dynamics at each site, within both the low- and middle-alpine belts, were characterized by similar rules within different quantities: most pronounced at the sub-surface (T–1), slightly decreas-

ing towards the air, and nearly extinct within the substrate layer due to its conservative thermal regime. Consequently, best correlations were found between T+200 ↔ T+15 (mean r^2 of 0.86), and T+15 ↔ T–1 (mean r^2 of 0.82), respectively. On the contrary, absolute temperatures were badly represented, as indicated by RMSE greater than 1.2. Furthermore, T+200 could not be used to represent T–1 or T–15 (mean r^2 of

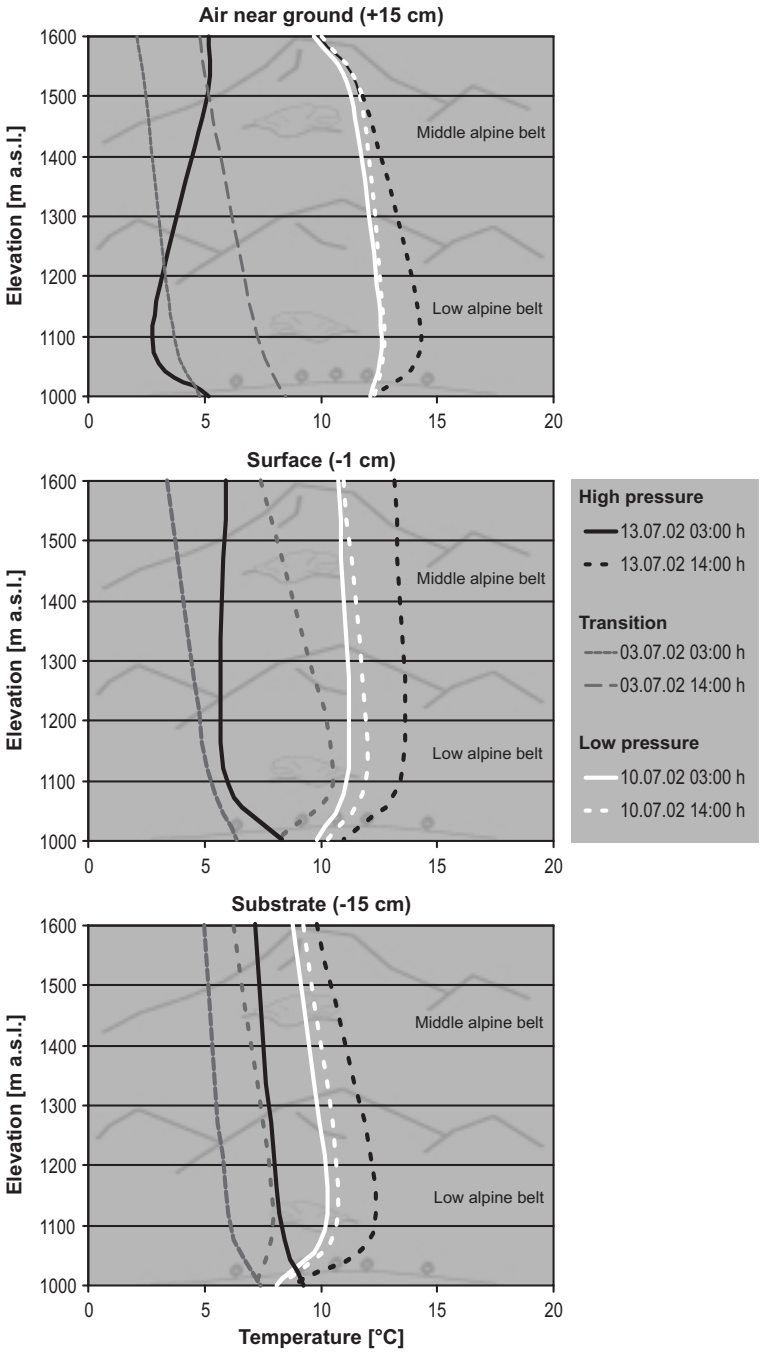

Fig. 5: General results of adiabatic temperature lapse rates during different summer weather situations for near-surface temperatures (Orig.)

Generalisierte Ergebnisse zum adiabatischen Temperaturgradient während verschiedener sommerlicher Wetterlagen für oberflächennahe Temperaturen

0.67 and 0.44 with RMSE ≥ 1.9 and 2.1). In fact, the temperature regime of the substrate was not at all represented by the other layers due to its smooth curvature induced by retarded heating and cooling. Worst representation was found within the low-alpine depressions as a result of water-saturated organic substrates.

Micro-scale results

3.3.1 Middle-alpine temperatures at different sites

The air temperature T+15 at all sites within the middle-alpine belt was highly correlated, indicated by r^2 greater than 0.96 and low RMSE of ≤ 1.0. This result accorded with generally high wind speeds at all sites even during cloudless high pressure weather situations. T+15 during the summer did not distinguish the differences of site conditions.

Using T–1 and T–15, respectively, we found higher biases in the correlation between the ridge sites on the one hand and slopes and depressions on the other. High soil moisture in the depressions and negative influence of shadowed conditions in northern exposures caused higher biases, as found while comparing slopes and depressions. Both sub-surface and substrate reacted with an r^2 of 0.83–0.86 and an RMSE of 1.28–1.87. On the contrary, the correlation of T–1 and T–15 between slopes and depressions was found to be very high: $r^2 \geq 0.96$; and RMSE of 1.13 for sub-surface, 0.44 for substrate conditions, respectively. In general, middle-alpine ridges showed warmer sub-surface and substrate conditions due to a lower substrate moisture than slopes and depressions. The difference in temperature dynamics of T–1 and T–15 between all sites was most decisive.

3.3.2 Low-alpine temperatures at different sites

Similar to the middle-alpine belt, T+15 at all sites showed high correlations, indicated by r^2 greater than 0.96 and low RMSE of ≤ 1.6. This result pointed to effective mixing processes despite lower wind speeds in the low-alpine belt. Also here, T+15 during the summer did not distinguish the differences of site conditions.

Again, we found higher biases in the correlation between the ridge sites on the one hand and slopes and depressions on the other. High soil moisture combined with organic substrates in the depressions and negative influence of shadowed conditions in northern exposures caused higher biases, as found while comparing slopes and depressions. The sub-surface reacted with an r^2 of 0.85–0.89 and an RMSE of 1.07–1.38. Regarding the substrate layer, differences were even more pronounced with r^2 of 0.47 and RMSE of 2.14 (A–B), and r^2 of 0.58 and RMSE of 1.87 (A–C), respectively. The correlation of T–1 and T–15 between slopes and depressions was found to be slightly higher: $r^2 \geq 0.71$; and RMSE of 1.54 for sub-surface, 0.44 for substrate conditions. Again, the ridges showed generally warmer sub-surface and substrate conditions with pronounced dynamics due to a lower substrate moisture than slopes and depressions. These behaved quite similarly, but were differentiated according to their substrate conditions (mineral – organic). The difference in temperature dynamics of T–1 and T–15 between all sites was most decisive.

3.4 Meso-scale results – altitudinal gradients

The correlation of T+15 curvature at the sites A–B–C between the low- and middle-alpine belts was found with an accuracy of > 84%; but high RMSE of 1.96–3.00 pointed to an insufficient representation of absolute temperatures. The high correlation indicated that overlying weather conditions, like passing frontier systems that control cloudiness, radiation etc., influenced the reaction of micro-climate with similar intensity without pronounced modification according to site properties. The high biases with altitude could be explained by the adiabatic lapse rate. But its deviation of ± 0.9 K from the general adiabatic lapse rate of –0,6 $K/100m^{-1}$ pointed to a complex daily variation of micro-climatic conditions with altitude induced by the overlying weather situation (nocturnal development of inversions etc.).

The synchronicity of curvature between T–1 was found with a r^2-value of 0.76 at the ridges; 0.62 in the depressions; and 0.48 on the slopes. Consequently, overlying weather conditions did not influence the reaction of micro-climate with similar intensity at different altitudes, i.e., the reaction was modified according to site differentiations. This fact had to be expected from micro-spatial results (lower correlation of T–1 between different sites). Thus, the response of the sub-surface to weather conditions was complex. The varying lapse rate of up to ± 1.3 K from the mean value –0.4 $K/100m^{-1}$ could not be explained by the weather situation only, but by micro-climatic variability along site differentiations. North-exposed slopes of different altitudes for instance differed according to percentage of vegetation cover that was found to be > 90% in low-alpine belt and < 30% in the middle-alpine belt, respectively.

Like the sub-surface, the substrate layer of different sites was not influenced with similar intensity by the overlying weather situation. The synchronicity of cur-

vature between T–15 was found with a r^2-value of 0.93 at the ridges; 0.80 in the depressions; and 0.54 on the slopes, all controlled by site-dependent differentiations. Thus, best correlation with lowest RMSE was found between the similar ridges, whereas worst correlation was found between depressions according to the different conditions regarding hydrology and substrate. The lapse rate was found to be in good concordance with the general adiabatic lapse rate of –0.6 K/100m^{-1}, with variations of ± 0.5 K, only.

Figure 5 exemplifies the lapse rates of temperature along the altitudinal gradient for different overlying weather situations. During low pressure weather situations, all near-surface layers at the ridges showed no differences in temperature between night and day. The low-alpine belt tended to be warmest compared with higher altitudes and the birch forest below, due to global radiation not hindered by fog or dense canopy of trees. Thus, temperatures in all layers increased from the sub-alpine to the low-alpine belt and slightly decreased towards higher elevations (air layer: –0.3 K/100m^{-1} due to effective turbulent mixing during windy periods). During transitional weather situations, the lapse rate was found to be in best concordance to the general adiabatic lapse rate of –0.6 K/100m^{-1}, during both nights and days. Extreme conditions were found during high pressure weather situations expressed by T+15 in the low-alpine belt. Highest daily and lowest nocturnal values were measured with an amplitude of 12 K. Compared with the ridges of the middle-alpine and sub-alpine belts daily values were at least 2 K higher at noon and 2 K colder before sunrise. We interpreted this phenomenon with differentiated spatial inversion patterns, sheltering barriers of the densely structured forest-line against cold air streams, and shading effects of the tree canopy layer. We also measured highest daily T–1 and T–15 values during high pressure weather situations, whereas sub-surface temperatures were identical in the low- and middle-alpine belt during days and nights. Obviously, altitude affected neither intense radiative heating nor inversion cooling at the ridges. Substrates reacted differently showing cooler conditions with altitude, but no daily amplitude in the forests. The difference between similar sub-surface but reduced substrate heating in the middle-alpine belt compared with the low-alpine phenomena was explained by higher substrate moisture in higher elevations, affecting thermal properties of substrate. Substrate temperatures in the forests did not show any daily amplitude during all different weather situations. All in all, summer temperature conditions could not be differentiated in total values along altitudinal gradients. We found similar minima in the low- and middle alpine belts, but during different weather situations. Highest summer temperatures were found in the low-alpine belt, but middle-alpine conditions were often much warmer than those of the forests.

4 Discussion

4.1 Across scale: vertical profiles – site differentiations – altitudinal gradients

In comparison with modelled vertical temperatures profiles, the extraordinary biases from meteorological standard data showed that environmental conditions near-ground differ from overlying climatic circulation patterns described by WALLÉN (1975). Quantifying the differences between general assumptions and meteorological predictions of T+200, and the eco-climatic conditions of T+15, T–1, and T–15, we showed that sub-surface and substrate conditions could not be predicted sufficiently, or even transferred from standard meteorological data. Near-surface temperatures at all different sites showed extremely high biases from the T+200. T+15 was poorly represented by T+200 (high RMSE), but had acceptable synchronicity. Over and above that, regarding higher temporal resolutions instead of long-term means, we found increasing deviation of temperatures from the adiabatic lapse rate. All in all, the extraordinary differences at all scales led us to conclude that the ecosystem determination is in situ enforced by micro-climatic conditions apart from meteorological trends. The complexity of the vertical energetic profile of near-surface conditions was now taken as to represent the superior determinant for ecosystem functioning. This was plausible according to the previous assumptions, since we could correlate vegetation patterns with micro-climate (LÖFFLER 2003). The results could help to densify the net of available vertical temperature profiles that are rare for northern high mountain landscape (WIELGOLASKI 1975; BLISS et al. 1981).

The above-stated problem of representing vertical temperature differentiation by means of meteorological standard data was reinforced regarding the spatial micro-scale. It was shown that near-surface air layers could not be used to explain differences in sub-surface and substrate temperatures among different sites during the observed representative summer period. The air temperature behaved similarly ($r^2 \geq 0.96$, RMSE $\leq$ 1.0), whereas sub-surface and substrate temperatures differed extraordinarily as a result of site-dependent thermal properties (LÖFFLER 2002a).

Approaches based on adiabatic lapse rate calculations (WHITEWAY et al. 1995) were found to be limited,

at least according to a high temporal resolution of daily temperature variations, but in most cases also according to differentiation of various weather situations. The approach to assess altitudinal gradients based on the adiabatic lapse rate of temperature could be used to generalize mean summer conditions over weeks. As such, our results do not touch general climatologic features of high mountains (BARRY 1992). We showed that micro-climatic phenomena were not expressed by the general mean conditions. The altitudinal gradient differed over diurnal and nocturnal time spans and resulted in complex temperature constellations. These had been found decisively to affect the environmental conditions of alpine plant life (CHAPIN a. SHAVER 1985). Furthermore, a group of higher alpine species were proved to be negatively correlated with high summer temperatures (DAHL 1998; GOTTFRIED et al. 1999). Temperature limit curves for species based on average temperatures of warmest and coldest months (HINTIKKA 1963; MOEN 1999) were used for geographical generalization, but proved to be unacceptable for ecological explanations. Thus, average values should not be used to characterize site conditions, but allow the potential of broad-scale distribution patterns to be calculated and interpreted.

SHAVER et al. (1986) had demonstrated that average growth on the long term was correlated with long-term average temperature, whereas inter-annual variations in temperature and growth were not at all correlated. KÖRNER et al. (1986) proved that the root-zone substrate temperature along a forest – grassland altitudinal transect was consistently higher under a low structured vegetation than under forest. HAVRANEK (1972) had pointed out that the substrate temperature might affect tree growth along the tree-line, which was the basic assumption for the hypothesis on tree-line determination by KÖRNER (1999). These assumptions were supported by our measurements. Moreover, similar results of substrate temperatures – plant life correlations, contributed earlier, stressed the importance of extreme environmental conditions (LÜDI 1938; BLISS 1956; MOSER et al. 1977).

4.2 Ecosystem complexity

There is no doubt about alpine ecosystems being complex in structure and micro-spatial diversity patterns (CHAPIN a. KÖRNER 1995; MOLAU 2003). The general assumptions to interpret these mosaics were causal descriptions (BILLINGS 1973; MOLENAAR 1987; ISARD a. BELDING 1989; STANTON et al. 1994). Moreover, substrate temperature variations had been found to be responsible for diurnal changes in CO_2 efflux. Over the course of the day sub-surface temperatures, measured as T–1, had been found to be best correlated with respiration activity (NADELHOFFER et al. 1991; OBERBAUER et al. 1992). We used those suggestions in a long-term project and analysed differences between low- and middle-alpine vegetation throughout different catchments. We discussed the correlations between the data sets of plant species composition with our micro-climatic results. The analysis showed that none of the different factors completely determined the vegetation along altitudinal gradients. Soil moisture was found with high significance, but did not explain species diversity patterns of the well-drained sites. Different clusters of plant species compositions were found along several vectors. The strongest correlation between vegetation and micro-climate was ruled by the number of days with sub-surface freeze-thaw processes, expressed by daily T–1 variations between –1 and +1° C. These conditions were found more frequently with increasing altitude. By way of contrast, maximum sub-surface temperatures correlated with specific groups of plant species most frequently found in early low-alpine snow beds. The two combined vectors indicated that the altitudinal change of vegetation was closely correlated with local sub-surface temperature attributes. These results proved that the high mountain ecology of plant species was most decisively determined by specific site conditions (LÖFFLER 2003). Since our simple model enabled the calculation of near-surface energetic constellations with high temporal resolution, we could easily predict near-surface temperature variations in small catchments (LÖFFLER a. WUNDRAM 2001; LÖFFLER a. PAPE 2003).

5 Conclusions

We conclude that high mountain ecosystems are determined by complex near-surface temperature gradients. These are not feasible with standard approaches like interpolation of meteorological standard data based on the adiabatic lapse rate, or statistics. Instead, intensive measurements or simple modelling approaches are needed for sufficient representation of micro-climatic conditions. We were able to calculate temperature variations with high spatial and temporal resolution using a very simple approach compared with common SVAT applications. The measurements used to describe the local energy balance were helpful to understand ecosystem functioning. They were necessary to calibrate the model for different site conditions. Biases between our data and general adiabatic models were clearly expressed by different purposes they

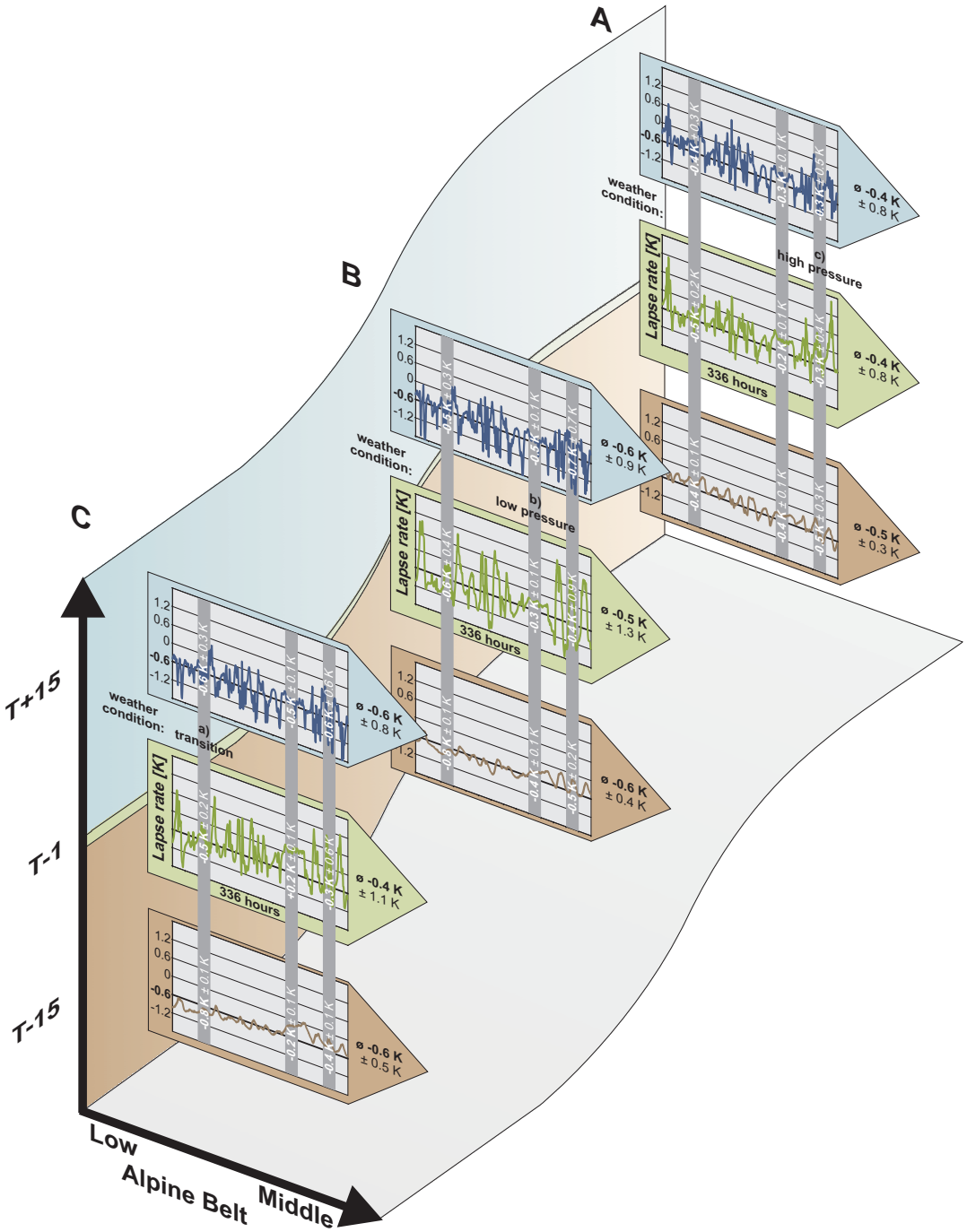

Fig. 6: Scheme of across spatio-temporal scale temperature gradients in alpine landscapes. The variation of near-surface temperatures (T+15, T–1, T–15) at different sites was expressed by the deviation of the adiabatic lapse rate against meteorological standards (T+200) over a characteristic summer period of 336 hours. Representative transitional (a), low pressure (b) and high pressure (c) weather situations were regarded separately. Finally, mean and standard deviation with altitude were summed up along the gradient of the alpine belts (Orig.)

Schema skalenübergreifender raum-zeitlicher Temperaturgradienten in alpinen Landschaften. Die Variation der oberflächennahen Temperaturen an verschiedenen Standorten ist mit Hilfe ihrer Abweichungen vom adiabatischen Gradienten gegen meteorologische Standards über eine 336-stündige Sommerperiode ausgedrückt. Repräsentative Übergangs-, Tiefdruck- und Hochdruckwetterlagen werden separat betrachtet

should by applied to. The adiabatic lapse rate (e.g., WHITEWAY et al. 1995) was found to agree with average calculations, but proved to be useless for predicting high resolution micro-climatic phenomena. Complex site conditions were expressed and summarized by complex thermal properties (Fig. 6). The altitudinal gradient [K/100 m] of T+15, T–1 and T–15 at ridges (A), northern exposure (B) and depression (C) showed pronounced amplitudes around the adiabatic lapse rate of –0.6 K/100 m, which was best represented by the substrate layer. Short term, the diurnal and nocturnal deviations showed characteristic curvatures for representative weather situations which best fit to the adiabatic lapse rate among transitional weather situations. Long term, the mean altitudinal lapse rate of temperature for each individual layer was well represented by the adiabatic lapse rate, but its standard deviation quantified deviations from this general assumptions.

We bridged the gap between intensive measurements for parameterization of SVAT models (i.e., CAYROL et al. 2000) and general models with our new simple energy balance model that was based on few input variables only. Since the model was run with high accuracy, we succeeded in proving its applicability for further ecosystem research.

Within the discussion of climate change (i.e., HOUGHTON et al. 1990) the sensitive high mountain ecosystems could act as indicators for ecosystem response to global warming (BENISTON a. INNES 1998; ELIASSEN a. GRAMMELTVEDT 1990). This may induce a change of species distribution and biodiversity in high mountain landscapes (CALLAGHAN et al. 1993) and finally lead to a replacement of alpine by sub-alpine ecosystems (CRAMER 1997), respectively. Thus, based on our results we are concerned that the prediction of high resolution temperature conditions for specific sites is necessary to understand the complex local interactions of plant species and environment.

Acknowledgments

The NORWEGIAN METEOROLOGICAL INSTITUTE has kindly supported this study with data from official stations. Furthermore, the authors thank their collaborators Annette Bär, Karsten Everth, Dr. Oliver-D. Finch, Bianca Hellbusch, Nora Lange, Jürgen Naujok, Ulrike Pöhlmann, Ole Rößler, Barbara Schmid and Dr. Dirk Wundram at the University of Oldenburg, Germany, and Prof. Dr. Anders Lundberg at the University of Bergen, Norway. Special thanks to the Norwegian locals, land owners, and authorities in Stranda and Vågå county.

References

ARNOLD, J. G.; SRINIVASAN, R.; MUTTIAH, R. S. a. WILLIAMS, J. R. (1998): Large area hydrologic modeling and assessment part I: model development. In: J. Am. Water Resour. Assoc. 34, 73-89.

BARRY, R. G. (1992): Mountain weather and climate. London.

BASTIAN, O. a. STEINHARDT, U. (eds.) (2002): Development and perspectives of landscape ecology. Dordrecht.

BENISTON, M. a. INNES, J. L. (eds.) (1998): The impacts of climate variability on forests. Berlin.

BILLINGS, W. D. (1973): Arctic and alpine vegetations: similarities, differences, and susceptibility to disturbance. In: Bio. Science 23, 697–704.

BLISS, L. C. (1956): A comparison of plant development in microenvironments of arctic and alpine tundras. In: Ecol. Monogr. 26, 303–337.

BLISS, L. C.; HEAL, O. W. a. MOORE, J. J. (eds.) (1981): Tundra ecosystems: A comparative analysis. IBP 25. Cambridge.

BOULET, G.; CHEHBOUNI, A.; BRAUD, I.; VAUCLIN, M.; HAVERKAMP, R. a. ZAMMIT, C. (2000): A simple water and energy balance model designed for regionalisation and remote sensing data utilization. In: Agric. For. Meteorol. 105, 117–132.

BRONSTERT, A. a. PLATE, E. J. (1997): Modelling of runoff generation and soil moisture dynamics for hill slopes and micro-catchments. In: J. Hydrol. 198, 177–195.

BRONSTERT, A.; MENZEL, L.; MIDDELKOOP, H.; DE ROO, A. P. a. VAN BEEK, E. (eds.) (2001): River basin research and management: integrated modelling and investigation of land-use impacts on the hydrological cycle. In: Phys. Chem. Earth 26, 487–640.

BRUSE, M. (1999): Die Auswirkungen kleinskaliger Umweltgestaltung auf das Mikroklima. Entwicklung des prognostischen numerischen Modells *ENVI-met* zur Simulation der Wind-, Temperatur- und Feuchteverteilung in städtischen Strukturen. Dissertation. Bochum. http://www-brs.ub.ruhr-uni-bochum.de/netahtml/HSS/Diss/BruseMichael/diss.pdf

BRUSE, M. a. FLEER, H. (1998): Simulating surface-plant-air-interactions inside urban environments with a three dimensional numeric model. In: Environmental Software and Modelling 13, 373–384.

CALLAGHAN, T.; SØMME, L. a. SONESSON, M. (1993): Impacts of climate change at high latitudes on terrestrial plant and invertebrates. Research report for the DN. Trondheim.

CAYROL, P.; KERGOT, L.; MOULIN, S.; DEDIEU, D. a. CHEHBOUNI, A. (2000): Calibrating a coupled SVAT vegetation growth model with remotely sensed and surface temperature. A case study for the HAPEX-Sahel grassland site. In: J. Appl. Meteorol. 39, 2452–2472.

CHAPIN, F. S. a. SHAVER, G. R. (1985): Individualistic growth response of tundra plant species to manipulated light, temperature and nutrients in a field experiment. In: Ecology 66, 564–576.

CHAPIN, F. S. a. KÖRNER, C. (eds.) (1995): Arctic and alpine biodiversity: patterns, causes and ecosystem consequences. Berlin.

CRAMER, W. (1997): Modelling the possible impact of climate change on broad-scale vegetation structure. Examples from northern Europe. In: OECHEL, W. C.; CALLAGHAN, T.; GILMANOV, T.; HOLTEN, J. I.; MAXWELL, B.; MOLAU, U. a. SVEINBJÖRNSSON, B. (eds.): Global change and arctic terrestrial ecosystems. In: Ecological Studies 124, 312–329.

DAHL, E. (1956): Rondane. Mountain vegetation in south Norway and its relation to the environment. In: Skr. Norske vidensk.-akad. Mat.-naturvid. kl. 3, 1–374.

– (1986): Zonation in arctic and alpine tundra and fellfield ecobiomes. In: POLUNIN, N. (ed.): Ecosystem theory and application. Chichester, 35–62.

– (1998): The phytogeography of northern Europe (British Isles, Fennoscandia and adjacent areas). Cambridge.

DENBY, B.; GREUELL, W. a. OERLEMANS, J. (2002): Simulating the Greenland atmospheric boundary layer. Part I: Model description and validation. Tellus 54A, 512–528.

DE VRIES, D. A. (1975): Heat transfer in soils. In: DE VRIES, D. A. a. AFGAN, N. H. (eds.): Heat and mass transfer in the biosphere I. Transfer processes in plant environment. Washington DC, 5–28.

ELIASSEN, A. a. GRAMMELTVEDT, A. (1990): Scenarios (2x CO_2 in Norway). Letter to the Ministry of Environment 01.02.1990. Oslo.

FÆGRI, K. (1972): Geo-ökologische Probleme der Gebirge Skandinaviens. In: TROLL, C. (ed.): Geoecology of the high-mountain regions of Eurasia: Proceedings of the symposium of the International Geographical Union, commission on high-altitude geoecology, November 20–22, 1969 at Mainz in connection with the Akademie der Wissenschaften und der Literatur in Mainz, Kommission für Erdwissenschaftliche Forschung. Erdwissenschaftliche Forschung 4. Wiesbaden, 98–106.

FLEAGLE, R. G. a. BUSINGER, J. A. (1963): Atmospheric physics. International geophysics series 5. New York.

FLEMING, M. D.; CHAPIN, F. S.; CRAMER, W.; HUFFORD, G. L. a. SERREZE, M. C. (2000): Geographic patterns and dynamics of Alaskan climate interpolated from a sparse station record. In: Global Change Biol. 6, 49–58.

FLÜGEL, W.-A. (1996): Hydrological response units (HRUs) as modelling entities for hydrological river basin simulation and their methodological potential for modelling complex environmental systems. Results from the Sieg catchment. In: Die Erde 127, 43–62.

FREMSTAD, E. (1997): Vegetationstyper i Norge. Norsk institutt for naturforskning, Temahefte 12. Trondheim.

FU, P. a. RICH, P. M. (1999): Design and implementation of the Solar Analyst: an ArcView extension for modeling solar radiation at landscape scales. Proceedings of the 19th Annual ESRI User Conference. San Diego, USA. http://www.esri.com/library/userconf/proc99/proceed/papers/pap867/p867.htm

GEIGER, R. (1961): Das Klima der bodennahen Luftschicht. Braunschweig.

GJÆREVOLL, O. (1990): Alpine plants. In: BERG, R. Y.; FÆGRI, K. a. GJÆREVOLL, O. (eds.): Maps of distribution of Norwegian vascular plants II. Trondheim.

GOTTFRIED, M. H.; PAULI, H.; REITER, K. a. GRABHERR, G. (1999): A fine-scaled predictive model for changes in species distribution patterns of high mountain plants induced by climate warming. In: Diversity and Distributions 5, 241–251.

HANKS, R. J. a. ASHCROFT, G. L. (1980): Applied soil physics. Soil water and temperature applications. Berlin.

HARDING, R. J.; GRYNING, S.-E.; HALLDIN, S. a. LLOYD, C. R. (2001): Progress in understanding of land surface/atmosphere exchanges at high latitudes. In: Theor. Appl. Climatol. 70, 5–18.

HAVRANEK, W. (1972): Über die Bedeutung der Bodentemperatur für die Photosynthese und Transpiration junger Forstpflanzen und für die Stoffproduktion an der Waldgrenze. In: Angew. Botanik 46, 101–116.

HINTIKKA, V. (1963): Über das Großklima einiger Pflanzenareale in zwei Klimakoordinatensystemen dargestellt. In: Ann. Bot. Soc. zool. Fenn. Vanamo 34.

HOUGHTON, J. T.; JENKINS, G. J. a. EPHRAUMS, J. J. (eds.) (1990): Climate change. The IPCC scientific assessment report prepared for IPCC by working group I, and accompanying policymakers` summary. Cambridge.

HUGGETT, R. J. (1995): Geoecology. An evolutionary approach. London.

HUTCHINSON, M. F. (1995): Interpolating mean rainfall using thin plate smoothing splines. In: International Journal for Geographical Information Systems 9, 385–403.

ISARD, S. A. a. BELDING, M. J. (1989): Evapotranspiration from the alpine tundra of Colorado, USA. In: Arct. Alp. Res. 21, 71-82.

JANSSON, P.-E. a. KARLBERG, L. (2001): Coupled heat and mass transfer model for soil-plant-atmosphere systems. Royal Institute of Technology, Dept of Civil and Environmental Engineering. Stockholm. ftp://www.lwr.kth.se/CoupModel/CoupModel.pdf

JONES, H. G.; POMEROY, J. W.; WALKER, D. A. A. a. HOHAM, R. W. (eds.) (2001): Snow ecology. An interdisciplinary examination of snow-covered ecosystems. Cambridge.

KALLIOLA, R. (1939): Pflanzensoziologische Untersuchungen in der alpinen Stufe Finnisch-Lapplands. In: Ann. Bot. Soc. Zoo. Bot. Fenn. Vanamo 13.

KERSTEN, M. S. (1949): Thermal properties of soils. Inst. of Technology, Eng. Exp. Station, Bull. 28, Univ. Minnesota, MN.

KÖHLER, B.; LÖFFLER, J. a. WUNDRAM, D. (1994): Problems of local geoecovariance in the central Norwegian mountains. In: Norsk Geogr. Tidsskr. 48, 99–111.

KÖRNER, C. (1995): Alpine plant diversity. A global survey and functional interpretations. In: Ecological Studies 113, 45–62.

– (1999): Alpine plant life. Functional plant ecology of high mountain ecosystems. Berlin.

KÖRNER, C.; BANNISTER, P. a. MARK, A. F. (1986): Altitudinal variation in stomatal conductance, nitrogene content and leaf anatomy in different plant life forms in New Zealand. In: Oecologica 69, 577–588.

KONDRATYEV, K. Y. (1969): Radiation in the atmosphere. International geophysics series 12. New York.

KRYSANOVA, V.; WECHSUNG, F.; BECKER, A.; POSCHENRIEDER, W. a. GRÄFE, J. (1999): Mesoscale ecohydrological modelling to analyse regional effects of climate change. In: Environ. Mod. Assess. 4, 259–271.

KUDO, G.; NORDENHÄLL, U. a. MOLAU, U. (1999): Effects of snowmelt timing on leaf traits, leaf production, and shoot growth of alpine plants: comparison along a snowmelt gradient in northern Sweden. In: Ecosience 6, 439–450.

LESER, H. (1997): Landschaftsökologie. Stuttgart.

LÖFFLER, J. (2002a): Altitudinal changes of ecosystem dynamics in the central Norwegian high mountains. In: Die Erde 133, 155–186.

– (2002b): Landscape complexes. In: BASTIAN, O. a. STEINHARDT, U. (eds.): Development and perspectives of landscape ecology. Dordrecht, 58–68.

– (2003): Micro-climatic determination of the vegetation along topographical, altitudinal, and oceanic-continental gradients in the central Norwegian high mountains. In: Erdkunde 57, 232–249.

– (2004): Snow cover, soil moisture, and vegetation ecology in central Norwegian mountain catchments. In: Hydrological Processes (accepted).

LÖFFLER, J. a. PAPE, R. (2003): Simulation des Energiehaushalts in mittelnorwegischen Hochgebirgslandschaften. In: LINDEMANN, R.; PRIEBS, A.; STEINECKE, K. a. VENZKE, J.-F. (eds.): Beiträge zur geographischen Nordeuropaforschung. Norden 15. Bremen, 221–233.

LÖFFLER, J. a. WUNDRAM, D. (2001): Räumliche und zeitliche Differenzierung des Temperaturhaushalts von Hochgebirgsökosystemen. In: GLÄSSER, E.; LINDEMANN, R.; PRIEBS, A. a. VENZKE, J.-F. (eds.): Nordica V. Aktuelle Beiträge zur Human- und Physiogeographie Nordeuropas. Norden 14. Bremen, 85–102.

– (2003): Geoökologische Untersuchungen zur Prozessdynamik mittelnorwegischer Hochgebirgsökosysteme. Oldenburger Geoökologische Studien 2. Bibliotheks- und Informationssystem, Oldenburg.

LÜDI, W. (1938): Mikroklimatische Untersuchungen an einem Vegetationsprofil in den Alpen von Davos III. In: Ber. Geobot. Inst. ETH, Stif. Rübel, 29–49.

MAY, D. E. (1976): The response of alpine tundra vegetation in Colorado to environmental modification. PhD thesis, University of Colorado, Boulder.

MITCHELL, G.; GRIGGS, R. H.; BENSON, V. a. WILLIAMS, J. (1997): Documentation of the EPIC-model. http://www.brc.tamus.edu/epic/documentation/index.html

MOEN, A. (1999): National atlas of Norway: vegetation. Hønefoss.

MOLAU, U. (2003): Overview: patterns in diversity. In: NAGY, L.; GRABHERR, G.; KÖRNER, C. a. THOMPSON, D. B. A. (eds.): Alpine diversity in Europe. Berlin, 125–132.

MOLENAAR, J. G. D. (1987): An ecohydrological approach to floral and vegetational patterns in arctic landscape ecology. In: Arct. Alp. Res. 19, 414–424.

MOSER, W.; BRZOSKA, W.; ZACHUBER, K. a. LARCHER, W. (1977): Ergebnisse des IBP-Projekts „Hoher Nebelkogel 3184". In: Sitzungsber. Österr. Akad. Wiss. Math.-Naturwiss. Kl. Abt. 1, 186, 387–419.

MOSIMANN, T. (1985): Untersuchungen zur Funktion subarktischer und alpiner Geoökosysteme (Finnmark [Norwegen] und Schweizer Alpen). In: Physiogeographica 7, 1–488.

MYKLESTAD, Å. (1993): The distribution of Salix species in Fennoscandia. A numerical analysis. In: Ecography 16, 329–344.

NADELHOFFER, K. J.; GIBLIN, A. E.; SHAVER, G. R. a. LAUNDRE, J. A. (1991): Effects of temperature and substrate quality on element mineralization in six arctic soils. In: Ecology 72, 242–253.

NEEF, E. (1967): Die theoretischen Grundlagen der Landschaftslehre. Gotha.

NOPPEL, H. a.. FIEDLER, F. (2002): Mesoscale heat transport over complex terrain by slope winds – A conceptual model and numerical simulations. Bound-Layer In: Meteor. 104, 73–97.

NORWEGIAN METEOROLOGICAL INSTITUTE (1991–2002): Yearly rapports – daily values. Climate data of 60300 Geiranger, 605000 Tafjord (Møre og Romsdal), 14550 Prestulen, 14580 Vågåmo – N.Grindstugu, 16740 Kjøremsgrende (Oppland). Oslo.

OBERBAUER, S. F.; GILLESPIE, C. T.; CHENG, W.; GEBAUER, R.; SALA SERRA, A. a. TENHUNEN, J. D. (1992): Environmental effects on CO_2 efflux from riparian tundra in the northern foothills of the Brooks Range, Alaska, USA. In: Oecologica 92, 568–577.

OKE, T. R. (2001[2]): Boundary layer climates. Reprint London.

OTTESEN, P. S. (1996): Niche segregation of terrestrial alpine beetles (Coleoptera) in relation to environmental gradients and phenology. In: J. Biogeography 23, 353–369.

PÅHLSSON, L. (1994): Vegetationstyper i Norden. TemaNord 1994: 665. Copenhagen.

PAPE, R. a. LÖFFLER, J. (2004): Modelling spatio-temporal near-surface temperature variation in high mountain landscapes. In: Ecol. Mod. 178, 483–501.

PRICE, M. F. a. BARRY, R. G. (1997): Climate change. In: MESSERLI, B. a. IVES, J. D. (eds.): Mountains of the world. A global priority. New York, 409–445.

RUMMUKAINEN, M.; RÄISÄNEN, J.; BRINGFELT, B.; ULLERSTIG, A.; OMSTEDT, A.; WILLEN, U.; HANSSON, U. a. JONES, C. (2001): A regional climate model for northern Europe: model description and results from the downscaling of two GCM control simulations. In: Clim. Dyn. 17, 339–359.

SCHELDE, K. (1996): Modelling the forest energy and water balance. ISVA series paper 62. Lyngby.

SHAVER, G. R. a. JONASSON, S. (1999): Response of arctic ecosystems to climate change: results of long-term field experiments in Sweden and Alaska. In: Polar. Res. 18, 245–252.

SHAVER, G. R.; CHAPIN, F. S. a. GARTNER, B. L. (1986): Factors limiting growth and biomass accumulation in *Eriopho-*

rum vaginatum L. in Alaskan tussock tundra. In: J. Ecol. 74, 257–278.

STANTON, M. L.; REJMANEK, M. A. a. GALEN, C. (1994): Changes in vegetation and soil fertility along a predictable snowmelt gradient in the Mosquito Range, Colorado, USA. In: Arct. Alp. Res. 26, 364–374.

TANNER, C. B. (1967): Measurement of evapotranspiration. In: Agronomy 11, 534–574.

VIRTANEN, R.; OKSANEN, L. a. RAZZHIVIN, V. (1999): Topographical and regional patterns of tundra heath vegetation from northern Fennoscandia to the Taimyr Peninsula. In: Acta Bot. Fenn. 167, 29–83.

WALKER, D. A.; BILLINGS, W. D. a. MOLENAAR, J. G. D. (2001): Snow – vegetation interactions in tundra environments. In: JONES, H. G.; POMEROY, J. W.; WALKER, D. A. a. HOHAM, R. W. (eds.): Snow ecology. An interdisciplinary examination of snow-covered ecosystems. Cambridge, 266–324.

WALLÉN, C. C. (ed.) (1970): Climates of northern and western Europe. World survey of climatology 5. Amsterdam.

WHITEWAY, J. A.; CARSWELL, A. I. a. WARD, W. E. (1995): Mesospheric temperature inversions with overlying nearly adiabatic lapse rate: An indication of a well-mixed turbulent layer. In: Geophysical Research Letters 22, 1201–1204.

WIELGOLASKI, F. E. (ed.) (1975): Plants and microorganisms. Fennoscandian tundra ecosystems 1. Ecological Studies 16. Berlin.

WITHERS, M. A. a. MEENTEMEYER, V. (1999): Concepts of scale in landscape ecology. In: KLOPATEK, J. M. a. GARDNER, R. H. (eds.): Landscape ecological analysis. Issues and applications. New York, 205–252.

Scale-specific matrices for the evaluation of temperature variation along nano-scale vertical profiles at single sites (I: T+200, II: T+15, III: T-1, IV: T-15), micro-scale topographical gradients between different sites (A: ridge, B: northern exposure, C: depression), and meso-scale altitudinal gradients over ecological belts (using both II, III, IV, and A, B, C) (Orig.).

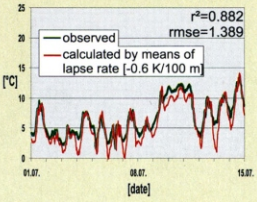

Middle Alpine Belt

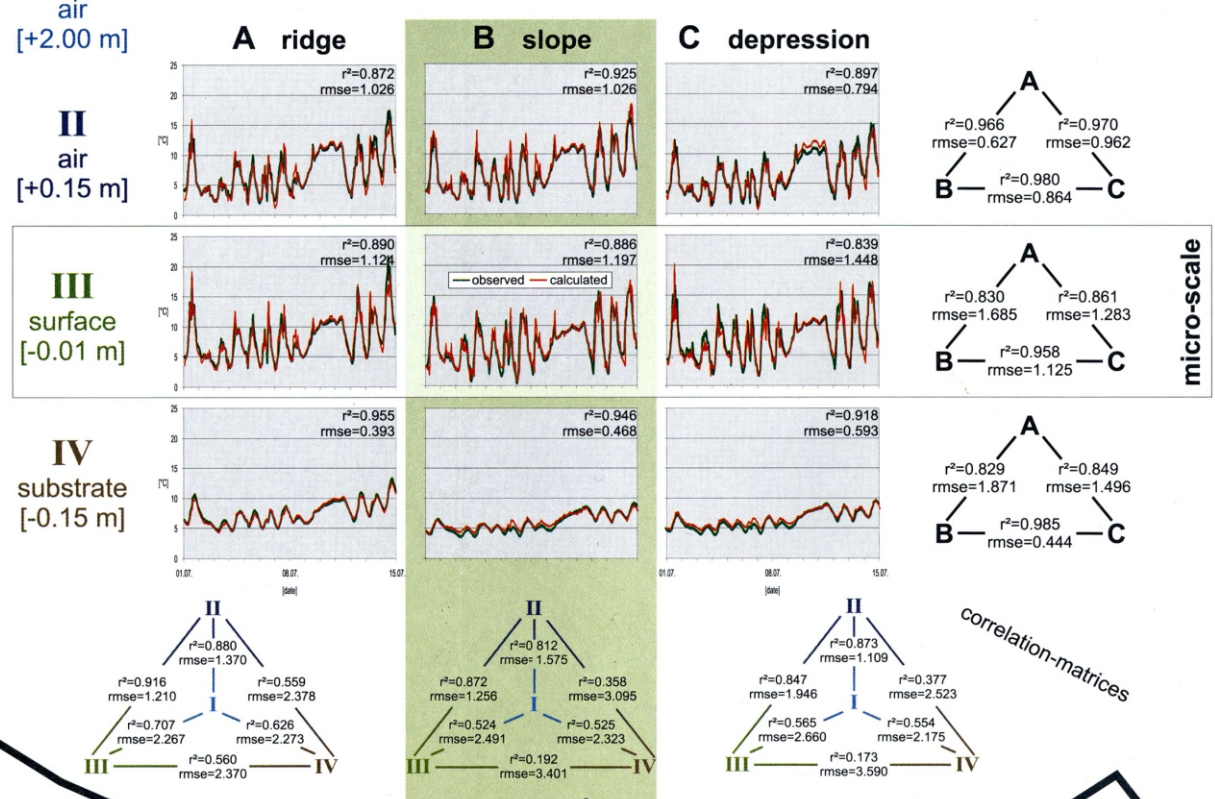

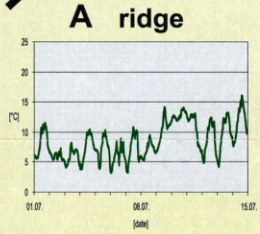

Low Alpine Belt

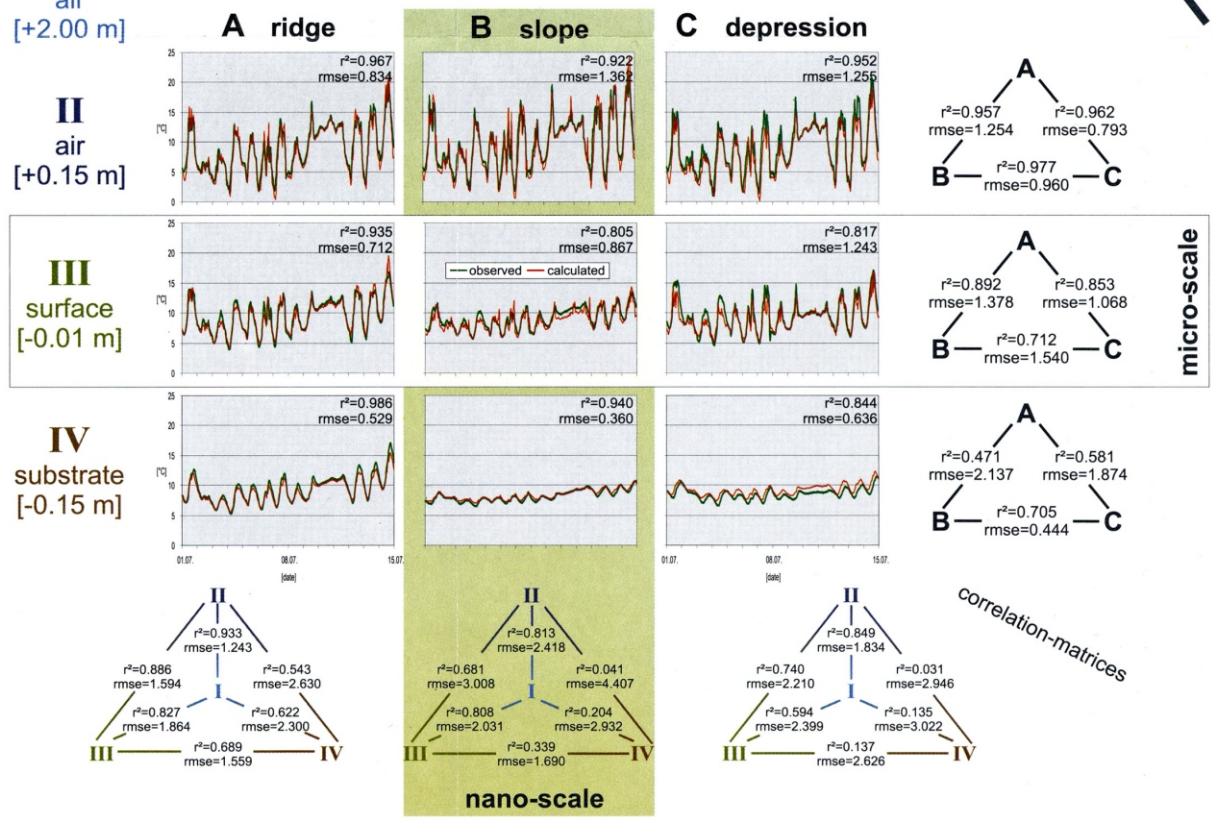

meso-scale

		A	B	C
II	r²	0.837	0.841	0.859
	rmse	2.180	2.996	1.955
III	r²	0.765	0.478	0.618
	rmse	2.207	3.230	3.000
IV	r²	0.925	0.798	0.540
	rmse	1.957	2.400	2.446

correlation-matrix